In Situ Determination of the Structural Properties of Initially Deposited Polyelectrolyte Multilayers

ARTICLE *in* LANGMUIR · FEBRUARY 2000

Impact Factor: 4.46 · DOI: 10.1021/la990650k

6 AUTHORS, INCLUDING:

Guy Ladam
Université de Rouen
23 PUBLICATIONS **1,127** CITATIONS
SEE PROFILE

Frédéric Cuisinier
Université de Montpellier
200 PUBLICATIONS **3,213** CITATIONS
SEE PROFILE

In Situ Determination of the Structural Properties of Initially Deposited Polyelectrolyte Multilayers

G. Ladam,[†,‡] P. Schaad,[§] J. C. Voegel,*[,‡] P. Schaaf,[†,⊥] G. Decher,[†] and F. Cuisinier[‡]

Institut Charles Sadron (CNRS-ULP), 6, rue Boussingault, 67083 Strasbourg Cedex, France, Fédération de Recherche "Odontologie" U424 INSERM-ULP, 11, rue Humann, 67085 Strasbourg Cedex, France, Institut Universitaire de Technologie, Université R. Schuman, 72, route du Rhin, 67400 Illkirch-Graffenstaden, France, and École Européenne de Chimie, Polymères et Matériaux de Strasbourg, 25, rue Becquerel, 67087 Strasbourg Cedex 2, France

Received May 27, 1999. In Final Form: September 20, 1999

The buildup of the first layers of a polystyrenesulfonate (PSS)/polyallylamine (PAH) multilayer is studied in situ by means of streaming potential measurements (SPM) and by scanning angle reflectometry (SAR). The results are discussed in the framework of a schematic representation of the multilayer in three zones: a precursor zone (I), a core zone (II), and an outer zone (III). This view seems to be supported by our experimental findings. The ζ potential of the multilayer determined by the SPM shows a symmetrical and constant charge inversion during the multilayer buildup. This seems to indicate an exact charge compensation in zone II and an excess charge that is entirely located in the outer zone III. It is also shown by SAR that a regular buildup regime, in which the thickness increment per layer is constant, is reached after the deposition of the first six polyelectrolyte layers, which gives an indication of the extension of zone I. The influence of the salt concentration C_{NaCl} present in the polyelectrolyte solutions during multilayer buildup is also investigated. It is found that an increase of the salt concentration in the polyelectrolyte solutions leads to larger amounts of deposited polyelectrolytes and to thicker multilayers. The amount deposited per polyelectrolyte layer δQ (PSS or PAH) is correctly predicted by the law $\delta Q = a \cdot C_{NaCl}^{\alpha} + b$ where α lies between 0.05 and 0.15. In addition, when a multilayer built up in salty solutions is brought in contact with pure water, it expands, indicating that the rinsing step mainly affects zone III of the multilayer, which appears thus to behave like a polyion layer. The structural changes of the multilayer consecutive to the replacement of the salt solution by pure water occur with characteristic times ranging from a few tens of minutes to several hours depending on the initial salt concentration. Finally, it is also found that the structural modifications of the film are fully reversible so that the initial multilayer structure is recovered when water is replaced again by the initial salt solution.

I. Introduction

Multilayers formed by the alternated adsorption of anionic and cationic polyelectrolytes proved to constitute an excellent and original way for the synthesis of ultrathin functional films.[1,2] The ease of their formation and the possibility to include specific molecules, proteins, or particles into the layers offer almost infinite possible film architectures.[2−4] Numerous studies were thus devoted to understanding the buildup of these multilayers. In general they are simply formed by an alternate dipping of the supporting surface into solutions of anionic and cationic polyelectrolytes, the layers being afterward rinsed with pure water or buffer and dried with nitrogen before being again immersed into the solution. The multilayer thickness seems then to increase linearly with the number of constituting pairs of polyanion/polycation. The number of pairs that can be adsorbed seems almost infinite so that very large film thicknesses are reachable.[5]

More precisely, we regard the basic structure of a multilayer film as subdivided into three zones (Figure 1). The first layers being deposited close to the substrate, they will possess a slightly different structure as the region of "bulk" film (core zone or zone II). Typically the thickness per layer in zone I is slightly smaller than that in zone II.[6,7] In zone II film properties are constant. When approaching the outer part of the multilayer, the local properties should again vary because of the solution environment.[2] The outer region over which the local film properties are no longer similar to those in zone II constitutes the outer zone of the film, or zone III. It should be clear that the transitions between zones I and II and between zones II and III are gradual. When the film is fabricated, zone I is completed first. As more layers are added zones I and III will preserve their respective thicknesses while zone II will grow in thickness. One could describe this in the following way: the new layer will adsorb on the surface, and thus the transition zone between II and III will move up by one layer as well. While zone II should be zwitterionic in nature, it should swell when exposed to salt solutions as the salt will break ionic

* To whom correspondence should be addressed. Phone: (33) 3 88 24 33 95. Fax: (33) 3 88 24 33 99. E-mail: jcv@odont3.u-strasbg.fr.
† Institut Charles Sadron.
‡ U424 INSERM.
§ Université R. Schuman.
⊥ École Européenne de Chimie, Polymères et Matériaux de Strasbourg.

(1) Decher, G.; Hong, J. D.; Schmitt, J. *Thin Solid Films* **1992**, *210/211*, 831−835.
(2) Decher, G. *Science* **1997**, *277*, 1232−1237.
(3) Knoll, W. *Curr. Opin. Colloid Interface Sci.* **1996**, *1*, 137−143.
(4) Laschewsky, A. *Eur. Chem. Chronicle* **1997**, *2*, 13−24.
(5) Lvov, Y.; Decher, G.; Möhwald, H. *Langmuir* **1993**, *9*, 481.
(6) Lvov, Y.; Decher, G. *Cryst. Rep.* **1994**, *39*, 696.
(7) Lösche, M.; Schmitt, J.; Decher, G.; Bouwman, W. G.; Kjær, K. *Macromolecules* **1998**, *31* (25), 8893−8906.

10.1021/la990650k CCC: $19.00
Published on Web 11/20/1999

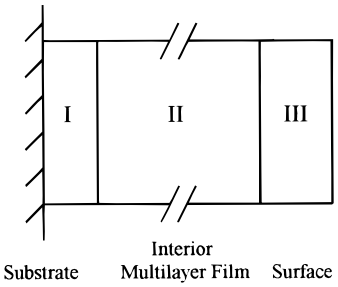

Figure 1. Schematic representation of a multilayer. Multilayer films can be subdivided into three regions: I, the region close to the substrate. This region is typically composed of only a few layers that are different from region II owing to the influence of the substrate. II, "bulk" multilayer film. Here all anionic layers possess equal thickness, and all cationic layers possess equal thickness. In most cases polyanion/polycation stoichiometry is observed to be 1:1 or at least close to that value. III, the region close to the surface of the film. This region is typically composed of only a few layers. It could be described as a transition zone between the charge-compensated region II and the charged surface. Please note that the transitions between regions I and II and between II and III are gradual and not as sharp as schematically depicted here.

bonds between polyanions and polycations.[8] In contrast, the layers in zone III should not be charge compensated and thus show classic polyion-like behavior. This means that they should swell in pure water and collapse in salt solutions owing to the screening of the electrostatic repulsion between charges of equal sign.

Most of the previous studies were carried out on dried films, and only few results have been reported in which multilayers were not dried after each step.[9−11] It is thus of interest to investigate in situ the properties and buildup of such multilayers. Moreover, the influence of water rinsing and drying steps in the formation process is not well characterized, and it would be of interest to better understand the response of the multilayer during these steps. Finally, polyelectrolytes are charged polymers and are thus sensitive to the ionic strength of the solution. Only few results were reported on the influence of this parameter on the structure of the multilayer. The aim of this study is thus to get new experimental data on the influence of all these parameters during the initial steps of the multilayer buildup.

We investigate the properties of the first deposited polystyrenesulfonate/polyallylamine (PSS/PAH) layers by means of scanning angle reflectometry (SAR) and streaming potential measurements (SPM). SAR gives access to the thickness and the mean refractive index of the multilayer in the presence of the solution,[12,13] and the SPM is sensitive to the ζ potential of the surface.[14] Our experimental results are discussed within the schematic three-zone representation of the multilayer. We analyze the influence of the ionic strength on the buildup of the polyelectrolyte film. Finally, we also study the relaxation of the films formed with solutions at different ionic strengths and which are suddenly brought in contact with pure water as is the case during the usual rinsing and drying procedures. To minimize influences induced by different ionic strengths in the deposition and rinsing solutions, we keep the ionic strength constant during deposition and only perform swelling/deswelling studies on completely assembled multilayers.

II. Materials and Methods

II. A. Materials. Anionic poly(sodium 4-styrenesulfonate) (MW = 70 000, cat. no.: 24,305-1) (PSS), cationic poly(allylamine hydrochloride) (M_n = 50000−65000, cat. no.: 28,322-3) (PAH) and cationic poly(ethyleneimine) (MW = 750 000, cat. no.: 18,197-8) (PEI) were purchased from Aldrich (Saint-Quentin-Fallavier, France), sodium chloride was purchased from Fluka (Saint-Quentin-Fallavier), and tris(hydroxyaminomethane) (Tris) was purchased from Sigma (Saint-Quentin-Fallavier). All the products of commercial origin were used without further purification. Ultrapure water (Milli-Q-plus system, Millipore, Bedford, MA) was used for the preparation of all buffers and solutions and for all the cleaning steps. The resistivity of the water was approximately 18.2 MΩ cm. The Tris-HCl buffer solution was prepared by adding 60.6 mg of Tris to 1 L of pure water (5×10^{-4} mol·L^{-1}). The pH was adjusted to 7.4 by addition of HCl in the solution.

II. B. Streaming Potential Measurements. Streaming potential measurements were used to determine the ζ potential of the multilayer. The experiments were performed on a homemade apparatus developed by Déjardin and co-workers.[14] It is composed of an electrophoresis capillary made out of fused silica with a radius of 530 ± 12 μm (tubing ref SIN 2042-R10, Perichrom SARL, Saulx-les-Chartreux, France) with lengths ranging from 18 to 23 cm, connected to two flasks on each side of the capillary. Each flask contains a reversible Ag/AgCl electrode used as a streaming potential sensor. The two electrodes are linked together through a voltmeter with a great internal impedance (Keithley 617 programmable electrometer). A pressure sensor calibrated in centimeters of water is also connected to both flasks. The pressure sensor and the two electrodes furnish, respectively, the pressure and potential differences on both sides of the capillary. The streaming potential is due to the streaming of the Tris-HCl buffer solution through the capillary by applying a high N_2 pressure on a third flask directly connected to the capillary. In a typical experiment, the water pressure rises up to 200 cm of water. The pressure difference, the flow rate through the capillary, and the streaming potential are directly recorded on a microcomputer. The ζ potential is related to the pressure difference ΔP and to the streaming potential (difference in the potential measured on the two Ag/AgCl electrodes) ΔV by the Smoluchovski relation:[15]

$$\Delta V = \Delta P \frac{\epsilon\epsilon_0 \pi R_c r^2 \zeta}{L\eta} \quad (1)$$

in which $\epsilon\epsilon_0$ is the permittivity of water (7.0×10^{-10} F/m at 20 °C), η represents the dynamic water viscosity (1.002×10^{-3} Pa·s at 20 °C), L is the length of the capillary and r its radius, R_c is the electrical resistance of the solution filled capillary (which is for our experiments typically of the order of 180 MΩ, and which is determined for each capillary), and ζ is the zeta potential of the capillary surface.

The experiments were conducted as follows:

(i) First the streaming potential of the bare capillary filled with Tris-HCl buffer was measured.

(ii) Then, a first layer of PEI was adsorbed from a PEI solution (PEI: 5 mg·mL^{-1}, 1 M NaCl). The capillary tube was filled with the polyelectrolyte solution with the help of a syringe, and the solution was kept in contact with the capillary for 15 min. The capillary was then extensively rinsed and equilibrated with Tris-HCl buffer. This procedure was necessary to reduce artifacts induced by the strong ionic strength of the solution containing the polyelectrolytes. The streaming potential was subsequently measured.

(8) Sukhorukov, G. B.; Schmitt, J.; Decher, G. *Ber. Bunsen-Ges. Phys. Chem.* **1996**, *100*, 948−953.
(9) Advincula, R.; Aust, E.; Meyer, W.; Knoll, W. *Langmuir* **1996**, *12*, 3536−3540.
(10) Kurth, D. G.; Osterhout, R. *Langmuir* **1999**, *15*, 4842−4846.
(11) Ramsden, J. J.; Lvov, Y. M.; Decher, G. *Thin Solid Films* **1995**, *254*, 246.
(12) Schaaf, P.; Déjardin, P.; Schmitt, A. *Langmuir* **1987**, *3*, 1131.
(13) Heinrich, L.; Mann, E. K.; Voegel, J. C.; Koper, G. J. M.; Schaaf, P. *Langmuir* **1996**, *12*, 4857.
(14) Zembala, M.; Déjardin, P. *Colloids Surf. B: Biointerfaces* **1994**, *3*, 119.
(15) Hunter, R. J. *Zeta Potential in Colloid Science*; Academic Press: New York, 1981.

(iii) A PSS layer was then built up from a PSS solution (PSS: 5 mg·mL^{-1}, 1 M NaCl) and the streaming potential measured by following a similar procedure as described in step ii.

(iv) Next a PAH layer was deposited from a PAH solution (PAH: 5 mg·mL^{-1}, 1 M NaCl) and the streaming potential measured by following the same procedure as in steps ii and iii.

(v) We then continued in a similar way to realize alternative PSS and PAH layer adsorptions and to measure, for each layer, the streaming potential. All the streaming potentials were determined in the same Tris-HCl buffer solution.

II. C. Scanning Angle Reflectometry (SAR) Experiments. Scanning angle reflectometry is an optical technique that allows one to obtain the optical thickness and the mean refractive index of a layer adsorbed on a tranparent solid (in our case silica, Suprasil, Heraeus, France). This technique is complementary with surface plasmon resonance spectroscopy (SPRS), which was also used to study the buildup of multilayers.[9,10] SAR requires one to work on a partially transparent interface (silica/water, for example), whereas SPRS requires one to work on a metallized surface (usually gold). Moreover, SAR allows one to obtain independently the optical thickness and the refractive index of the studied layer, and SPRS seems to be mainly sensitive to $(n_{lay} - n_{sol})L$, where $(n_{lay} - n_{sol})$ represents the difference between the refractive indexes of the layer and of the solution and L represents the optical thickness of the layer. By assuming a typical value of $(n_{lay} - n_{sol})$, one can then have a direct access to the layer thickness L. In SAR one measures the intensity of a reflected laser beam (in the present case HeNe, $\lambda = 632.8$ nm) by the solid/layer/solution interface as a function of the incidence angle around the Brewster angle (typically over an angular range of $\pm 1°$). The laser beam is thus polarized in the plane of incidence. The details of the apparatus and the technique can be found in refs 12 and 13. Assuming a refractive index profile for our layer, one finds the parameters characterizing the profile by adjusting the experimental intensity curves to the theoretical ones relative to the index profile. In SAR a maximum of three parameters can be determined,[16] and usually only two are really reachable. We used here the most common approach in which the profile of an homogeneous and isotropic optical monolayer was used. It is characterized by two parameters: an optical thickness L and a mean refractive index n_{lay} (we will usually not characterize the layer by n_{lay} but by $\Delta n = n_{lay} - n_{sol}$, where n_{sol} is the refractive index of the solution). A least-squares fitting procedure is used to determine these parameters, in which one minimizes the quantity

$$\chi^2 = \frac{1}{N_a}\sum_i \left(\frac{f^{exp}(\theta_i) - f^{mod}(\theta_i)}{0.01|f^{exp}(\theta_i) + \sigma_0} \right)^2 \qquad (2)$$

with respect to the profile parameters. The sum is performed over all the N_a angles θ_i at which the reflected intensity $f^{exp}(\theta_i)$ has been measured. $f^{mod}(\theta_i)$ corresponds to the calculated reflected intensity relative to the postulated refractive index profile, and σ_0 corresponds to the baseline noise or roundoff error. We used in our experiments $\sigma_0 = 0.05$. Typical reflectivity curves with their corresponding best fits are given in Figure 2.

Before an experiment was begun, the silica prism employed as substrate for multilayer film depositions was cleaned for 15 min at 90 °C with 0.01 mol·L^{-1} sodium lauryl sulfate (SDS) and extensively rinsed with ultrapure water. Then it was cleaned for 15 min at 90 °C with 0.1 mol·L^{-1} hydrochloric acid and finally extensively rinsed again with ultrapure water. Large amounts of NaCl solutions ranging from 0.01 to 0.9 mol·L^{-1} were prepared. Each polyelectrolyte solution was obtained by dissolving 750 mg of polyelectrolyte in 150 mL of NaCl solution. All the solutions were degassed under vacuum just before use.

The silica surface was first brought in contact with pure water, and the reflectivity curve corresponding to the Fresnel (abrupt density profile) silica/water interface was measured. The curve was used for calibration of the apparatus and for the measurement of the refractive index of water. Water was then replaced by an NaCl solution and the reflectivity curve determined again. This allowed us to verify the calibration of the apparatus and to measure the refractive index of the NaCl solution. We then began to build up the polyelectrolyte multilayer in the following way:

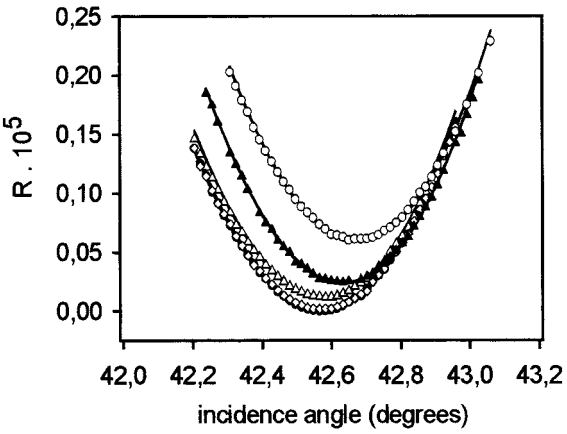

Figure 2. Typical reflectivity curves measured during the buildup of a multilayer in the presence of 0.75 mol·L^{-1} NaCl: (●) experimental Fresnel curve, (△) after PAH#1 layer, (◇) after PSS#2 layer, (▲) after PSS#3 layer, (○) after PAH#3 layer. One observes that after PSS#2 layer deposition the reflectivity curve becomes almost indistinghishable from the initial Fresnel curve. This suggests that the refractive index of the multilayer becomes equal to the one of our silica substrate. Full lines correspond to the fitted curves according to the homogeneous and isotropic layer model. For this experiment we found PSS#3, $L = 30.4$ nm, $\Delta n = 0.1325$; PAH#3, $L = 30.7$ nm, $\Delta n = 0.1396$.

(i) The NaCl solution was replaced by the PEI solution of same NaCl concentration. After 30 min of contact with the silica surface, the PEI solution was replaced by the NaCl solution. As expected the reflectivity changes due to the PEI layer were usually too small to be observed.

(ii) We then adsorbed alternatively PSS and PAH layers on the surface by using the same procedure as described for PEI (only the interaction time between the polyelectrolyte solution and the silica surface was taken to be 15 min instead of 30 min). All the PSS and PAH solutions contained the same NaCl concentration as the rinsing NaCl solution.

(iii) After the adsorption of 10 consecutive layers (5 PSS and 5 PAH, the last layer being PAH), the cell was rinsed with the NaCl solution and subsequently with pure water. The replacement of the NaCl solution by pure water took about 20 min, and no reflectivity measurements were performed during this operation. The layer was then kept in contact for several hours with pure water. During this period of time, the reflectivity curves were continuously determined at a rate of one curve every 7 min in order to follow the relaxation of the multilayer in pure water. The minimum relaxation times reachable with these experiments are thus of the order of 25 min.

(iv) Finally, after several hours, we again replaced water by the rinsing NaCl solution in order to investigate the reversibility of the structural changes of the multilayer. Reflectivity curves were again continuously determined for several hours.

III. Results and Discussion

Figure 3 shows typical results relative to the ζ potential of a multilayer ending alternatively with a PSS and a PAH layer. The first measured potential corresponds to that of the bare silica surface. Three experiments were performed. In all three experiments the ζ potential alternates in sign when passing from a multilayer ending with a polyanion to a multilayer ending with a polycation. This is consistent with the ζ potential measurements made by Caruso et al.[17] on PSS/PAH multilayers and by

(16) Heinrich, L.; Mann, E. K.; Voegel, J. C.; Schaaf, P. *Langmuir* **1997**, *13*, 3177.

(17) Caruso, F.; Donath, E.; Möhwald, H. *J. Chem. Phys. B* **1998**, *102*, 2011.

(18) Hoogeveen, N. G.; Stuart, M. A. C.; Fleer, G. J.; Böhmer, M. R. *Langmuir* **1996**, *12*, 3675−3681.

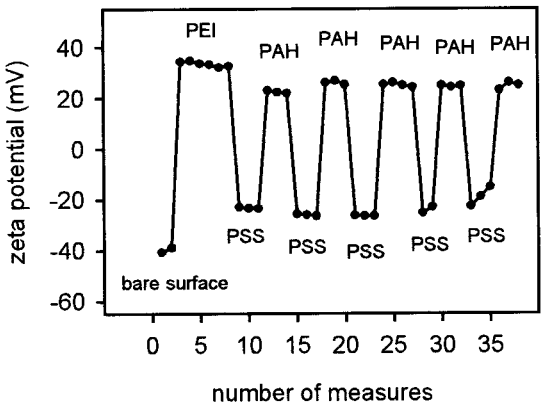

Figure 3. Typical evolution of the ζ potential during the buildup of a PSS/PAH multilayer from 5 mg·mL^{-1} polyelectrolyte solutions. The line has no physical meaning and was added to guide the eyes.

Hoogeveen et al.[18] on poly(vinylimidazol)/poly(acrylic acid) multilayers, both multilayers being deposited on colloidal particles and the ζ potential determined from the electrophoretic mobility of the particles. Moreover, we find that the potential alternates almost *symmetrically*, the absolute values of the ζ potentials remaining almost constant with the layer number. This indicates that, during the successive deposition of PSS and PAH polyelectrolytes, each polyelectrolyte always brings with it a net charge which is, in absolute value, the same for the polyanion and the polycation and thus does not change during the buildup procedure so that the charge excess of the multilayer does not vary between two consecutive PSS and PAH layers. It is reasonable to assume that the charge brought by each polyelectrolyte serves to compensate the excess charge of the multilayer leading to an uncharged zone II and to create a new excess charge of opposite sign located in zone III. The values of the ζ potential found for our experiments are typically of the order of −20 mV for the anionic outer layer and +20 mV for the cationic layer after the deposition of three to four layers. Caruso et al. found ζ potentials that were of the order of (30 ± 10) mV for the multilayers with a cationic outer layer and (−40 ± 10) mV with an anionic outer layer (see ref 17, Figure 2). The ζ potentials obtained by these authors are thus of the same order of magnitude as the ones found here with totally different substrate and measuring techniques.

A typical evolution of the optical thickness L, of the mean refractive index difference Δn, and of $\Delta n \cdot L$ with the number N of deposited layers is given in Figure 4a,b. $\Delta n \cdot L$ is, in first approximation, directly proportional to the amount of material forming the multilayer. It comes out that after the deposition of six polyelectrolyte layers (up to PSS#3), the optical thickness L and $\Delta n \cdot L$ increase linearly (within experimental error) with N and that Δn almost reaches a constant value. The linear increase of $\Delta n \cdot L$ with N is consistent with results obtained by X-ray reflectivity. The measurements were, however, performed on dried multilayers built on a precursor film made out of 10^{19} to 20^{5} initial layers. The linear increase of the film thickness is also in accordance with the observations made on hydrated films, without drying, by SPRS[9,10] and an optical wave guide technique.[11] Essler[20,21] made a similar

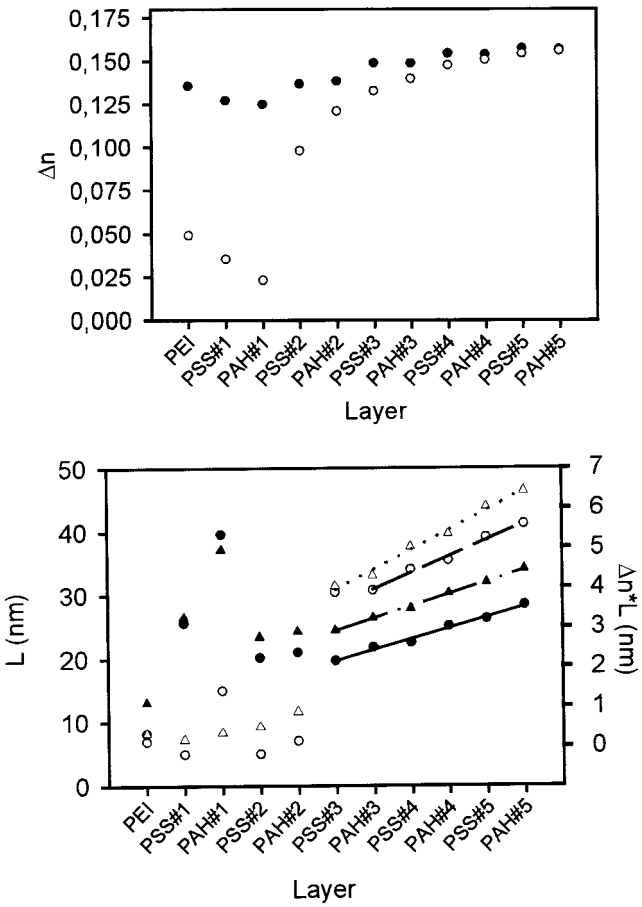

Figure 4. (a) Evolution of Δn during the buildup of a multilayer in the presence of 0.15 mol·L^{-1} NaCl (●) and 0.75 mol·L^{-1} NaCl (○). (b) Evolution of L (nm) and $\Delta n \cdot L$ (nm) during the buildup of a multilayer in the presence of 0.15 mol·L^{-1} NaCl (respectively ● and ▲) and 0.75 mol·L^{-1} NaCl (respectively ○ and △). Lines represent the linear regression of the linear part of the evolution. The slopes correspond, respectively, to 1.70 (—), 0.34 (—••—), 2.41 (— —), and 0.49 (•••).

observation when studying PSS/PAH multilayers deposited under a floating Langmuir monolayer of dimethyldioctadecylammoniumbromide (DODAB) by means of ellipsometry. In our experiments the reproducibility of the structural parameters of the first five or six deposited layers was quite poor. This can be due to the small differences between the reflectivity curves relative to the first layers and the Fresnel curve, which originate from the fact that the amount of adsorbed material on the surface is small and that the mean refractive index of some of these first layers can be very near to that of the silica. Moreover, the reproducibility of the cleaning procedure for all surfaces is certainly not perfect, and this can also influence the structure of the first adsorbed layers. This later is confirmed by the fact that even though the increments in L and $\Delta n \cdot L$ with the deposited layers become reproducible after the six initial layers, the absolute value of the thickness L of the multilayer can be offset from one experiment to another by up to 5 nm in the worst case, owing to the poor reproducibility of the deposition of the six initial layers (the typical thickness of a six-layer-thick multilayer ranges from 16 to 36 nm when the salt concentration of the polyelectrolyte solutions varies from 0.01 to 0.9 mol·L^{-1}). This also shows that *to reach the regular buildup regime of the multilayer one needs a*

(19) Lvov, Y.; Decher, G.; Sukhorukov, G. B. *Macromolecules* **1993**, *26*, 5396.

(20) Essler, F. Polyelectrolytadsorption an geladene Lipidmonolagen: Aufbau von Multischichten an der Wasser/Luft-Grenzfläche, Übertragung und Charakterisierung Thesis, Universität Mainz, 1998.

(21) Ruths, J.; Essler, F.; Decher, G.; Riegler, H. Manuscript in preparation.

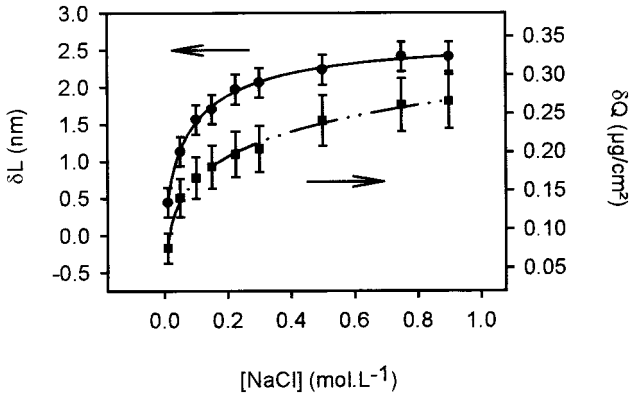

Figure 5. Variation of the mean thickness increase δL (●) and of the mean amount increase δQ (■) corresponding to the addition of a supplementary layer in the linear part of the multilayer buildup versus the NaCl concentration of the polyelectrolyte solutions. For δL the line (—) has no physical meaning and was added to guide the eye. For δQ the line (—··—) represents the approximation by a function of the type $\delta Q = aC_{\mathrm{NaCl}}^{\alpha} + b$. The error bars were determined from the relation $Q = (\Delta n \cdot L) \cdot (\mathrm{d}n/\mathrm{d}c)^{-1}$ with $\Delta[\delta(\Delta n \cdot L)] = 0.025$ nm and with the mean value $\mathrm{d}n/\mathrm{d}c = (0.197 \pm 0.016)$ mL·g^{-1} calculated from the results of Essler.[20,21]

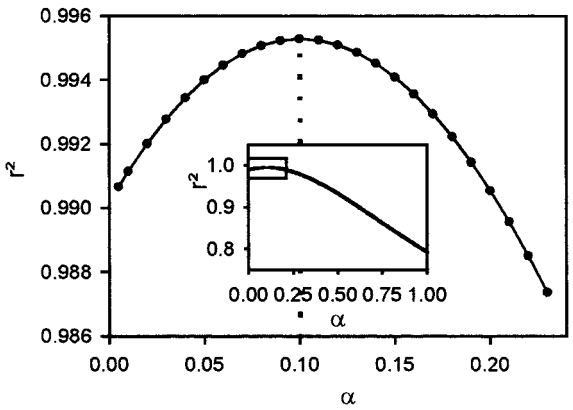

Figure 6. Variation of the linear regression coefficient $r^2(\alpha)$ of the curves $\delta Q = a \cdot C_{\mathrm{NaCl}}^{\alpha} + b$ obtained by maintaining the value of α constant ranging from 0.001 to 1 in the inset and from 0.001 to 0.25 for the main curve.

precursor film constituted by at least six polyelectrolyte layers (*three pairs of layers*) *for our substrate*. These first six layers seem thus to compose zone I of our multilayer, the layers located within the regular buildup regime corresponding to zones II and III.

Figures 5 and 6 show the evolution of the increments of the optical thickness δL and of the amount of polyelectrolyte δQ ($Q = (\Delta n \cdot L)(\mathrm{d}n/\mathrm{d}c)^{-1}$) due to the deposition of one layer as a function of the NaCl solution concentration. These increments were determined in the regular buildup regime. We used a mean value of 0.197 mL·g^{-1} for $\mathrm{d}n/\mathrm{d}c$ for both polyelectrolytes in solution[20,21] to determine Q. We observe an increase of both δL and δQ with the salt concentration of the buildup solutions. This is similar to the observations made on multilayers that were prepared with a drying step after each polyelectrolyte layer deposition.[5,22] Our results are also in accordance with those found by Essler.[20,21] They can be explained as follows: In a polyelectrolyte solution of low salt concentration, the chains take an extended and stiff conformation, whereas at high salt concentrations the polyelectrolyte chains look more like a dense globule because of charge screening. When the adsorption of the polyelectrolytes on a charged surface is performed at low salt concentrations, it should thus lead to thin layers in which the polyelectrolytes adopt a flat conformation. At higher salt concentrations, owing to charge screening the chain should adopt more extended conformations.[20,21] This should lead to higher amounts of polyelectrolytes and larger thicknesses of the deposited layers. In addition, at low salt concentrations, it is expected that the deposited layers should not lead to charge excesses on the surface that are too large.[23,24] Indeed, a large charge excess would lead to a high electric field that extends over large distances owing to the large value of the Debye length. This again would result in a large surface free energy owing to the electrostatic contribution. To obtain a small charge excess, starting from a bare charged surface, the system should adsorb amounts of polyelectrolytes just sufficient to compensate the initial surface charge of the substrate leading to a small charge excess after the deposition of the first polyelectrolyte layer. However, this excess charge constitutes the driving force for the deposition of the next polyelectrolyte layer. One thus expects smaller amounts of deposited polyelectrolytes at small salt concentrations during the buildup stage. We thus come to the conclusion that also for the case of minimal osmotic stress, *increased salt concentration in the polyelectrolyte solutions leads to higher amounts of adsorbed polyelectrolytes in the multilayers and to larger multilayer thicknesses*.

We have tried to relate δQ to the salt concentration C_{NaCl} of the buildup polyelectrolyte solutions by using the fitting function (see Figure 6a)

$$\delta Q = a \cdot C_{\mathrm{NaCl}}^{\alpha} + b \qquad (3)$$

a, b, and α being the fitting parameters. Such a power law dependence on C_{NaCl} is expected from theoretical considerations.[25] The best fit was obtained for $a = 0.53 \pm 0.16$ μg·cm^{-2}·L·mol^{-1}, $b = -0.25 \pm 0.16$ μg·cm^{-2}, and $\alpha = 0.10 \pm 0.04$. The negative value of b can be due to the large uncertainty on b and also to the rapid variation of δQ with C_{NaCl} in the small concentration domain. Figure 6 shows the linear regression coefficient $r^2(\alpha)$ of the curves $\delta Q = f(C_{\mathrm{NaCl}}^{\alpha})$ obtained by maintaining the value of α constant and ranging from 0.001 to 1. It is shown that α must lie in the range $0.05 \leq \alpha \leq 0.15$. Our experimental data are thus not compatible with the value $\alpha = 0.5$ found in refs 20 and 21.[20,21] Theoretical investigations are currently under way to determine the value of this exponent.[25]

Up to now the multilayers were always studied in solutions, the salt concentration being held constant all over the building procedure. However, when such a multilayer is suddenly brought in contact with pure water, ions contained in the layer may diffuse out of the multilayer into the water leading eventually to structural changes in the film. This process was followed by SAR. It is illustrated in parts a and b of Figure 7, which correspond to a typical experiment. In Figure 7a we represent the evolution of the mean refractive index of the multilayer, and in Figure 7b we show the evolutions of the optical thickness L and of $\Delta n \cdot L$ proportional to the fixed amount, as a function of time. To analyze the SAR curves it was always assumed that the multilayers behave as homo-

(22) Serizawa, T.; Takeshita, H.; Akashi, M. *Langmuir* **1998**, *14*, 4088.

(23) Joanny, J. F. *Eur. Phys. J. B* **1999**, *9*, 117.

(24) Böhmer, M. R.; Evers O. A.; Scheutjens, J. M. H. M. *Macromolecules* **1990**, *23*, 2288.

(25) Castelnovo, M.; Joanny, J. F. Private communication.

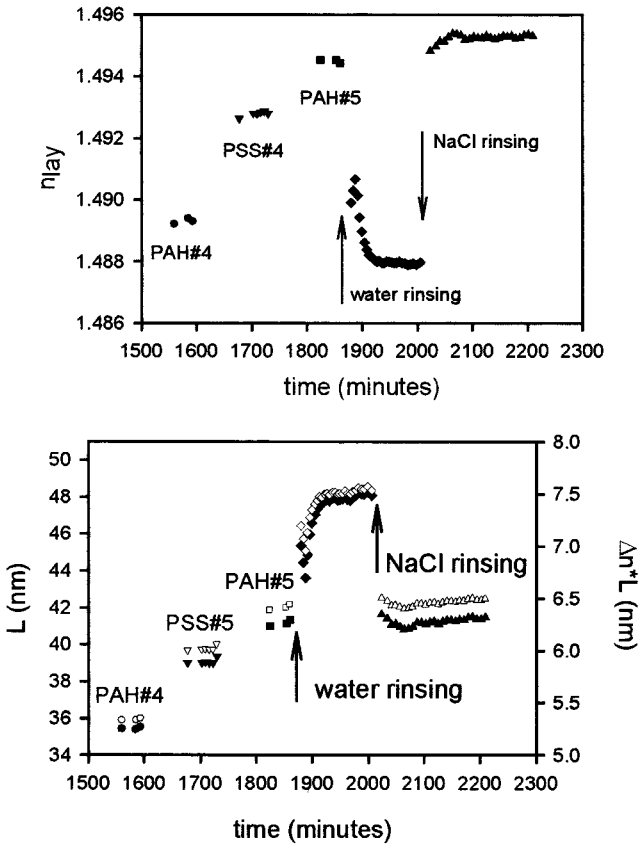

Figure 7. (a) Evolution of n_{lay} during a multilayer buildup in the presence of 0.75 mol·L^{-1}NaCl: (●) after addition of the layer PAH#4, (▼) after addition of the layer PSS#5 layer, (■) after addition of the layer PAH#5, (◆) after replacement of the 0.75 mol·L^{-1} NaCl solution that was in contact with PAH#5 by pure water, and (▲) after late replacement of pure water by the 0.75 mol·L^{-1} NaCl solution again. (b) Evolution of the optical thickness L(nm) (filled symbols) and of $\Delta n \cdot L$ (nm) (open symbols) of the multilayer under the same experimental conditions as for (a) (● and ○) after addition of layer PAH#4, (▼ and ▽) after addition of layer PSS#5, (■ and □) after addition of layer PAH#5, (◆ and ◇) after replacement of the 0.75 mol·L^{-1} NaCl solution that was in contact with PAH#5 by pure water, and (▲ and △) after a last replacement of pure water by the 0.75 mol·L^{-1} NaCl solution.

geneous and isotropic layers. In Figure 7a,b we plotted the three last steps of the buildup (addition of PAH#4, PSS#5, and PAH#5, measured in contact with the NaCl solution), the rinsing with pure water, and the final rinsing with the NaCl solution. After the rinsing with pure water it is found that both the refractive index and the layer thickness changed with the time of contact between the multilayer and pure water. The optical parameters seem to level off after a characteristic time t_s indicating a stabilization of the multilayer. After being brought again in contact with a NaCl solution of concentration equal to that used during the buildup procedure, the multilayer almost instantaneously recovered the optical parameters that characterized it at the end of the buildup procedure and before rinsing with pure water. *This procedure thus demonstrates that uptake and release of salt ions are totally reversible.* This too is consistent with the results of Essler[20,21] who found similar properties but with multilayers that were dried between two consecutive rinsings. The time t_s needed for the layer to stabilize in water varies with the salt concentration of the buildup solutions. In Figure 8 one observes that this time decreases when the salt concentration increases. It reaches a plateau at a value of the order of 1 h, in the present case, for a multilayer

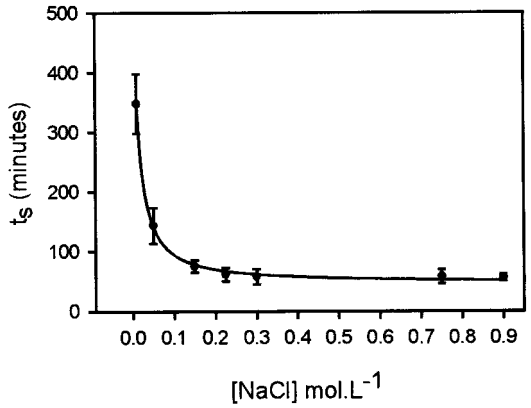

Figure 8. Variation of the relaxation time t_s (in minutes) after rinsing of the multilayer with pure water versus the NaCl concentration used to build up the multilayer. $t = 0$ corresponds to the start of the rinsing process. The solid line is added to guide the eye and has no physical meaning.

Table 1. Values of the Refractive Indexes of Water and NaCl Solutions Derived from the Fresnel Curves, and Values of the Optical Parameters L (nm) and n_{lay} of the Polyelectrolyte Multilayer before and after the Water-Rinsing Process

	$L \pm 0.4$ nm		$n_{sol} \pm 0.0005$		$n_{lay} \pm 0.0005$	
[NaCl] (mol·L^{-1})	PAH#5	water-rinsing plateau	water	NaCl solution	PAH#5	water-rinsing plateau
0.01				1.3319		
0.05	22.2	21.7	1.3312	1.3317	1.4857	1.4868
0.10				1.3328		
0.15	28.2	27.5	1.3320	1.3334	1.4904	1.4909
0.225	29.7	30.3	1.3323	1.3345	1.4910	1.4905
0.30	30.5	32.0	1.3316	1.3346	1.4918	1.4898
0.50				1.3370		
0.75	41.1	47.9	1.3312	1.3386	1.4945	1.4879
0.90	44.7	53.5	1.3313	1.3401	1.4942	1.4866

composed by 11 successive layers (1 PEI layer, 5 PSS layers, and 5 PAH layers). Moreover, the parameter changes, as expected, are larger at high salt concentrations. Indeed, the larger the buildup NaCl concentration, the higher the salt gradient when the multilayer is suddenly brought in contact with pure water, and it is expected that the ions diffuse out of the multilayer at a flux that should be proportional to this salt gradient. The characteristic reorganization time should thus be smaller for high buildup C_{NaCl} as is observed. From Table 1 it is shown that, except for the very lowest salt concentrations, which lead to rinsing effects remaining within experimental errors, the layer thickness significantly increases and the refractive index significantly decreases when the salt solution is replaced by pure water, which is characteristic for a swelling process. It is interesting to note that on one hand the multilayer thickness increases with the salt concentration of the buildup polyelectrolyte solutions as discussed above, but on the other hand, once the multilayer is built from a high salt concentration solution, its thickness increases significantly when the salt solution is replaced by pure water.

Within the three-zone picture, one expects a decrease of the thickness of zone II and a thickness increase of zone III after the replacement of the salt solution by pure water. Our results thus seem to indicate that, for our multilayers, zone III is much more affected by the rinsing than are zones I and II. This can be explained as follows: On one hand, the polyelectrolytes in zone III behave as polyions and dangle more or less into the solution. This zone is thus expected to swell after an ionic strength decrease in

the solution. On the other hand, zone II behaves more like polyzwitterions and should thus deswell by ionic strength reduction. But the polyelectrolytes in this zone are entangled and should even form charge complexes. It is thus expected that the relative swelling of zone III is larger than the deswelling of zone II. Moreover the overall swelling effect is also proportional to the thickness of the respective zones. Since zone II is relatively small, in our multilayers, the overall effect should be dominated by zone III as is observed. One should, however, be able to observe an opposite effect for larger multilayers.

Finally from Table 1 one can also note that $\Delta n \cdot L$ can increase during the water rinsing step. This seems at first sight nonphysical because $\Delta n \cdot L$ is, in first approximation, proportional to the amount of material in the layer. However, the refractive index increment dn/dc also changes with the salt concentration in the multilayer,[20,21] and the refractive index of the solution itself changes. These changes can be as large as 10% when the salt concentration varies from 0 to 1 mol·L^{-1}. Moreover, the structural changes of the multilayer can lead to associations or dissociations between PSS and PAH polyelectrolytes. This can also affect the mean value of dn/dc for the overall mixture of PSS and PAH. One should thus not draw too precise conclusions from this increase in $\Delta n \cdot L$. Finally, it must be mentioned that we do not have any explanation for the order of magnitude of the time scales involved in the reorganization of the multilayer when changing from a salt solution to pure water and for the fact that the restoring time is very short when bringing the multilayer again in contact with the initial salt solution.

IV. Conclusions

We have investigated the initial steps of multilayer deposition in situ. The polyions used here were PAH and PSS, the system with which the majority of previous experiments were performed and about which we currently know the most. ζ potential measurements show that the surface potential changes from negative to positive and back when polycations and polyanions are adsorbed. In addition, the ζ potentials relative to the multilayer when the last layer is formed by the polyanion and the polycation remain constant during the buildup once a regular regime is reached. Our experiments were performed in capillaries that are a quasi-planar SiO_2/SiOH surfaces and thus very close to the glass or silicon wafer substrates that are commonly used. The ζ potential measurements described here are furthermore in good agreement with similar results previously obtained on colloidal surfaces. Additionally we show that the sign of the surface potential also changes when the layers are deposited with a minimum of osmotic stress. For these same conditions (same ionic strength for deposition and rinsing solutions/no intermediate drying/in situ measurements), we show that increased ionic strengths lead to thicker films and that zone I (the layers between solid support and the core zone (zone II)) is composed of approximately six layers. Swelling experiments show that changes of ionic strength lead to reversible changes of film thickness. As of yet the swelling behavior cannot be deconvoluted for a precise quantitative analysis of each zone. The increase of layer thickness with a reduction of ionic strength seems, however, to be due to the expected swelling of zone III in pure water. Owing to principle restrictions in our setup, we were only able to get meaningful data for layer numbers 6−10. Thus we are currently limited to films in which zone II would be rather thin and should play only a negligible role in swelling. This is in agreement with the swelling behavior we have seen.

Acknowledgment. The authors thank CNRS and INSERM for financial support through the program "Adhésion Cellules-Matériaux". This work was performed within the framework of the Research Network "Mécanismes physicochimiques d'adhésion cellulaire: forces d'adhésion entre ligands et récepteurs biologiques".

LA990650K